# A Stochastic Model for Discrete Waves in the *Limulus* Photoreceptor

RICHARD SREBRO and MAHMOOD BEHBEHANI

From the Neurosensory Laboratory and the Department of Physiology, State University of New York at Buffalo, Buffalo, New York 14214

ABSTRACT A stochastic model that links the absorption of a photon to the production of a discrete wave in the photoreceptor of the lateral eye of *Limulus* is proposed. By separating a discrete wave into an initial component due directly to the absorption of a photon, and a second quasi all-or-nothing component, a mathematical description of the latencies of discrete waves is deduced and some important features of their time courses are suggested. The predictions of the model are compared to observations from 60 different ommatidia.

## INTRODUCTION

The ability to respond to the absorption of a single photon is a fundamental property of the photoreceptor cells of vertebrate and invertebrate animals (Hecht, Shlaer, and Pirenne, 1942; Reichardt, 1965). In the photoreceptor of the lateral eye of the horseshoe crab, *Limulus*, the response to a single photon can be observed as a transient discrete depolarization, called a discrete wave (for reviews of the evidence see Wolbarsht and Yeandle, 1967; Srebro and Yeandle, 1970). We propose a stochastic model that links the absorption of a photon to the production of a discrete wave.

## THEORY

Experimental evidence suggests that sodium is the most important ion involved in the production of photocurrent in the *Limulus* photoreceptor (Fuortes, 1959; Kikuchi, Naito, and Tanaka, 1962; Smith, Stell, and Brown, 1968; Millecchia and Mauro, 1969). We assume that the photoreceptor cell membrane has the general features of neuronal membrane and that a discrete wave reflects two processes: (*a*) an effect due directly to light, and (*b*) an effect due to depolarization. By treating the two processes separately, a mathematical description is derived that predicts the latencies of discrete waves, and suggests important features of their time course.

As a preliminary, consider that the voltage and time-dependent behavior

of the photoreceptor cell membrane is similar to axonal membrane, as described by Hodgkin and Huxley (1952). We infer that: (*a*) small depolarizations cause a small increase in the membrane's sodium conductance, analogous to the passive (or electrotonic) response of axonal membrane, (*b*) large depolarizations cause a large transient increase in sodium conductance, analogous to the all-or-nothing response of axonal membrane, and (*c*) the transition between the two types of sodium conductance change, (*a*) and (*b*) above, is critically dependent on the amount of depolarization.

In the remainder of this section we derive a mathematical model for the discrete wave process based on the analogy of the photoreceptor membrane to axonal membrane. The kernel of the model may be stated as follows. The direct effect of a photon absorption is to produce a spatially localized depolarization of small magnitude analogous to the electrotonic response of axonal membrane, and if the depolarization is sufficient a quasi all-or-nothing response is produced which then propagates along the photoreceptor membrane. We describe the direct effect of a photon absorption as a stochastic process, and its variability accounts for the variation of the latency of a discrete wave.

It is useful to define our model in terms of sodium channels, and to consider the effect of light on their behavior. A sodium channel is defined as a fixed channel through which sodium ions may pass. It is either fully open or fully closed. The number of sodium channels per unit area of membrane is finite. Let $R$ and $\bar{R}$ represent, respectively, the state of a visual pigment molecule before and after it has absorbed a photon. The two states are mutually exclusive, and transitions between them are instantaneous. A transition from $R$ to $\bar{R}$ may occasionally occur spontaneously. Assume that the molecules of visual pigment are part of the membrane structure (as suggested by Smith and Brown, 1966). Let $\beta$ be the rate at which sodium channels open and let $\mu$ be the rate at which sodium channels close. In general $\beta$ and $\mu$ depend on voltage and on time and their behavior accounts for the sodium conductance of the membrane.

Let all the visual pigment molecules be in state $R$ at time $t = 0$, and let $\beta = 0$. If a visual pigment molecule changes to state $\bar{R}$ at time $t = 0$, we assume that there is an instantaneous effect on the sodium channels in the vicinity of that molecule, such that $\beta$ becomes greater than zero. The effect on any particular sodium channel may depend on its physical distance from the visual pigment molecule that is in state $\bar{R}$, but we simplify by assuming the spatial distribution to be uniform over a group of $n_o$ sodium channels. Once a sodium channel opens, the membrane is slightly depolarized, and in general, the voltage and time-dependent properties of $\beta$ and $\mu$ become important. However, the behavior of the sodium conductance discussed in the

preliminary paragraph implies that $\beta$ and $\mu$ are only slightly affected by small depolarizations. To simplify, let the following restrictions apply:
(*a*) $\beta$ and $\mu$ are independent of voltage and time,
(*b*) sodium channels open and close independently, and
(*c*) the lifetime of $\bar{R}$ is infinite.
Let

$$h = \text{a small increment of time,}$$

and

$$n(t) = \text{number of sodium channels open at time } t.$$

Then

$$[\beta(n_o - n[t])h + o(h)] = \text{probability that a sodium channel opens during } h \text{ at } t,$$

and

$$[\mu n(t) + o(h)] = \text{probability that a sodium channel closes during } h \text{ at } t$$

where $o(h)$ represents terms that approach zero more rapidly than $h$ does. If $n_o$ is large, the first probability is approximately equal to $[\alpha h + o(h)]$, where $\alpha = n_o\beta$. Denoting by $p_n(t)$ the probability that $n$ sodium channels are open at time $t$, we write,

$$\begin{aligned} p_0(t + h) &= p_0(t)(1 - \alpha h) + p_1(t)\mu h \\ &\vdots \\ p_n(t + h) &= p_n(t)(1 - \alpha h - n\mu h) + p_{n-1}(t)\alpha h + p_{n+1}(t)(n + 1)\mu h \\ &\vdots \end{aligned} \tag{1}$$

(The set of equations given by (1) state that, in general, if $n$ channels are open at time $t + h$, this state may have had one of the following three histories:
(*a*) $n$ channels were open at $t$, and no channels opened or closed during $h$
(*b*) $n - 1$ channels were open at $t$, and one channel opened during $h$
(*c*) $n + 1$ channels were open at $t$, and one channel closed during $h$.)
Rearranging and dividing each equation above by $h$ and allowing $h \to 0$ gives:

$$\begin{aligned} p_0'(t) &= -p_0(t)\alpha + p_1\mu \\ &\vdots \\ p_n'(t) &= -p_n(t)(\alpha + n\mu) + p_{n-1}(t)\alpha + p_{n+1}(t)(n + 1)\mu \\ &\vdots \end{aligned} \tag{2}$$

with initial conditions,

$$p_0(0) = 1$$

$$p_n(0) = 0; \quad n \neq 0$$

where

$$p'_n(t) = d(p_n[t])/dt.$$

The infinite set of equations given by (2) can be solved for the mean value $\overline{n(t)}$ (Feller, 1957), and

$$\overline{n(t)} = \alpha/\mu(1 - \exp[-\mu t]) \tag{3}$$

If at any time $n(t)$ becomes large, then, by assumption, a transient increase in sodium conductance results. We infer that in this case sodium channels outside the group of $n_o$ open. That is, as a result of a critical depolarization, a propagated response is initiated, and the depolarization spreads along the membrane.

Let $m$ equal a critical value of $n(t)$ that corresponds to the critical depolarization. The latency of the propagated response is the (variable) time required for $n(t)$ to reach $m$ for the first time, after an $R$ to $\bar{R}$ transition at $t = 0$. Let all the restrictions apply as before, and denote by $Q_n(t)$ the probability that $m$ sodium channels are simultaneously open sometime during an interval of time $t$ given that $n$ channels are open at the beginning of the interval. Then for $m \neq 0$,

$$\begin{aligned}
&Q_0(t + h) = Q_0(t)(1 - \alpha h) + Q_1(t)\alpha h \\
&\vdots \\
&Q_n(t + h) = Q_n(t)(1 - \alpha h - n\mu h) + Q_{n-1}(t)n\mu h + Q_{n+1}(t)\alpha h; \quad 0 < n < m - 1 \\
&\vdots \\
&Q_{m-1}(t + h) = Q_{m-1}(t)(1 - \alpha h - [m - 1]\mu h) + Q_{m-2}(t)(m - 1)\mu h + \alpha h.
\end{aligned}$$

Rearranging and letting $h \to 0$,

$$\begin{aligned}
&Q'_0(t) = -Q_0(t)\alpha + Q_1(t)\alpha \\
&\vdots \\
&Q'_n(t) = -Q_n(t)(\alpha + n\mu) + Q_{n-1}(t)n\mu + Q_{n+1}(t)\alpha; \quad 0 < n < m - 1 \\
&\vdots \\
&Q'_{m-1}(t) = -Q_{m-1}(t)(\alpha + [m - 1]\mu) + (m - 1)\mu Q_{m-2}(t) + \alpha
\end{aligned} \tag{4}$$

with initial conditions,

$$Q_n(0) = 0; \quad n < m$$

where

$$Q_n'(t) = d(Q_n[t])/dt.$$

The system of $m$ equations, (4), are the first passage equations and their solution for $Q_0(t)$ gives the integral of the probability density function (*p.d.f.*) of the latency of the propagated response. If $\alpha$ is much greater than $\mu$, we can use the approximation

$$\begin{aligned}
&Q_0'(t) = -Q_0(t)\alpha + Q_1(t)\alpha \\
&\vdots \\
&Q_n'(t) = -Q_n(t)\alpha + Q_{n+1}(t)\alpha; \quad 0 < n < m - 1 \\
&\vdots \\
&Q_{m-1}'(t) = -Q_{m-1}(t)\alpha + \alpha.
\end{aligned}$$

Taking Laplace transforms of the $m$ equation above, and denoting the transformed variable as $s$,

$$\begin{aligned}
&(s + \alpha)Q_0(s) - \alpha Q_1(s) = 0 \\
&\vdots \\
&(s + \alpha)Q_n(s) - \alpha Q_{n+1}(s) = 0; \quad 0 < n < m - 1 \\
&\vdots \\
&(s + \alpha)Q_{m-1}(s) = \alpha/s.
\end{aligned}$$

The system of $m$ algebraic equations can be solved for $Q_0(s)$ using either Cramer's rule, or chain substitution, and

$$Q_0(s) = (1/s)(\alpha^m/[s + \alpha]^m). \tag{5}$$

Let $q_0(t) = d(Q_0[t])/dt \equiv$ *p.d.f.* of the latency. Then,

$$q_0(t) = \alpha^m t^{m-1} \exp(-\alpha t)/(m - 1)! \tag{6}$$

which is a gamma density with shape parameter $m$, and scale parameter $\alpha$.

We now relax the constraint that the lifetime of $\bar{R}$ is infinite, and assume instead that it is of the order of the latency of a propagated response. Thus, on occasion, the critical depolarization may not be reached at the instant of the transition from $\bar{R}$ to $R$, and a propagated response will not be initiated.

Assuming that for small depolarizations the observed membrane potential is proportional to $n(t)$, the following features of the shapes of discrete waves are suggested:

(*a*) There are two types of discrete waves, namely, propagated and nonpropagated, which are, respectively, large and small.

(*b*) A nonpropagated wave follows a time course, on the average, similar to

$\overline{n(t)}$ in equation (3) in its rising phase, and declines with exponential time constant $1/\mu$.

(*c*) A propagated wave may be preceded by a slow progressive depolarization. The terminal decline of a propagated wave represents the closure of sodium channels at a time when the membrane depolarization is of small magnitude. It is therefore identical with the decline of a nonpropagated wave, and has the same exponential time constant, $1/\mu$.

Finally, we consider that more than one photon may be absorbed in a brief flash of light. If each photon acts independently with regard to latency, it can be shown (Srebro and Yeandle, 1970) that the latency to the first discrete wave is given by

$$g(t) = (\lambda q_0[t] + M_d) \exp\left(-\int_0^t \lambda q_0[x]\, dx - M_d t\right) \qquad (7)$$

where

$g(t)$ = *p.d.f.* of the latency to the first discrete wave to follow a brief flash,
$\lambda$ = average number of light-induced discrete waves per flash,
$M_d$ = average rate at which spontaneous discrete waves occur.

These considerations imply that $\alpha$ may be estimated from the latencies of discrete waves, and $\mu$ from their time courses.

## METHODS

The experimental methods used were similar to those given in detail by Srebro and Yeandle (1970). The latency of the first discrete wave to follow a 10 msec flash of light was measured by dividing a fixed interstimulus interval (usually 5 sec) into a convenient number of subintervals (usually 250) and determining in which subinterval the first discrete wave began. Each stimulus presentation was called a trial. A block of trials was called a run (and ranged from 125 to 1000 trials). The last second of the interstimulus interval was assumed to be free of any effect of the stimulus. The following tabulations were made:

$T$ = interstimulus interval (seconds)
$\Delta t$ = subinterval duration (seconds)
$N$ = number of trials in a run
$N_S$ = number of trials on which at least one discrete wave began within the interval $(0, T - 1)$
$N_D$ = number of trials on which at least one discrete wave began in the last second of $T$
$n(k)$ = the number of trials on which the first discrete wave began in the $k^{\text{th}}$ subinterval following the stimulus, and $k$ ranged over the interval $(0, T - 1)$.

Equation (7) was written in the following incremental form for $k = 1$,

$$g(1) = \lambda q_0(1) + M_d \Delta t$$

and for $k > 1$,

$$g(k) = (\lambda q_0(k) + M_d \Delta t) \exp\left(-\sum_{j=1}^{k-1} \lambda q_0(j) - M_d \Delta t(k-1)\right)$$

where,

$k$ referenced the $k^{\text{th}}$ subinterval following the stimulus

$$M_d = \log_e (1 - N_D/N)$$

$$\lambda = \log_e (1 - N_S/N) - M_d(T - 1)$$

$$g(k) = n(k)/N$$

and solved iteratively for $q_0(k)$. The sum of the values of $q_0(k)$ over all the subintervals is one. Let,

$$z(k) = q_0(k)N(1 - \exp(-\lambda)). \tag{8}$$

The term, $z(k)$ is proportional to $q_0(k)$, the estimate of greatest interest. The constant of proportionality, $N(1 - \exp[-\lambda])$ is an estimate of the number of light-induced discrete waves observed in the run. The estimate, $z(k)$, is a better estimator to use for statistical analysis and curve fitting than is $q_0(k)$ because random variations are simply related to $z(k)$ but are not simply related to $q_0(k)$.

Some of the latency measurements were made by hand from penwriter records, but most of them were made as follows. An AC-coupled signal proportional to the cell depolarization was compared to an adjustable DC voltage level. The comparator output and the AC signal were displayed and the experimenter adjusted the DC voltage level so that the comparator changed state whenever the experimenter observed that a discrete wave began. The time that elapsed between the beginning of each stimulus and the first comparator transition that followed it was automatically measured, digitized, and recorded on magnetic tape. If no transition occurred in the interstimulus interval a special mark was inserted on the tape record. Trials on which no light was presented were intermingled among the light stimuli, and these were used to estimate $M_d$. Spontaneous discrete waves and discrete waves resulting from low levels of steady illumination were also recorded on analog tape.

The data reported here derive from observations on 60 ommatidia (57 retinula cells, and 3 eccentric cells). Latency measurements are reported for 33 cells (108 runs, approximately 50,000 trials). Latency measurements for 10 of these cells were reported in a previous study (Srebro and Yeandle, 1970).

Estimates of the parameters $\alpha$, and $m$, in equation (6) were made from the measurements, $z(k)$ for each run. The predicted values of $z(k)$ were calculated by writing equation (6) in incremental form, and substituting the resulting expression for $q_0(k)$ in equation (8). Thus each predicted value of $z(k)$ was given by the expression,

$$[\Delta t \alpha^m t^{m-1} \exp(-\alpha t)/(m - 1)!]N(1 - \exp[-\lambda]) \tag{9}$$

where $t$ corresponded to the midpoint of the $k^{\text{th}}$ subinterval. A nonlinear curve-fitting

procedure was used to adjust the parameters $\alpha$, and $m$ so as to minimize the sum of squares of the differences between observed and predicted values of $z(k)$. The method used was a modification of the steepest descent method (Draper and Smith, 1966). Initial parameter estimates were obtained by the maximum likelihood method of Markovic (1965). When the best simultaneous estimates of $m$ and $\alpha$ were found, a chi-square test was used to determine the goodness of fit. In 102 of 108 runs the fit was acceptable at the 5% level. The accuracy of the estimates of $\alpha$ an $m$ were examined by comparing replicate runs, *i.e.* runs on the same cell, at the same temperature, but taken at different times. Replicate runs were available for 23 cells. The fractional variation (standard error/mean) for the estimate of $m$ was 0.22, and the fractional variation of the estimate of $\alpha$ was 0.32.

## RESULTS

### *S and L waves in Retinula and Eccentric Cells*

Fig. 1 A shows 13 isolated discrete waves recorded in a retinula cell. By isolated we mean a single discrete wave that does not overlap other discrete waves in time. The figure was constructed by selecting the first 13 isolated discrete waves in the run and arranging them in the order of their appearance. Fig. 1 B shows nine isolated discrete waves recorded in an eccentric cell, and was constructed in the same way as Fig. 1 A. The records of Figs. 1 A and 1 B were taken from different ommatidia but at similar temperatures. The discrete waves shown are typical of their respective cell types.

Figs. 2 A and 2 B show peak amplitude histograms for discrete waves from the same two cells represented in the previous figure. Both histograms are

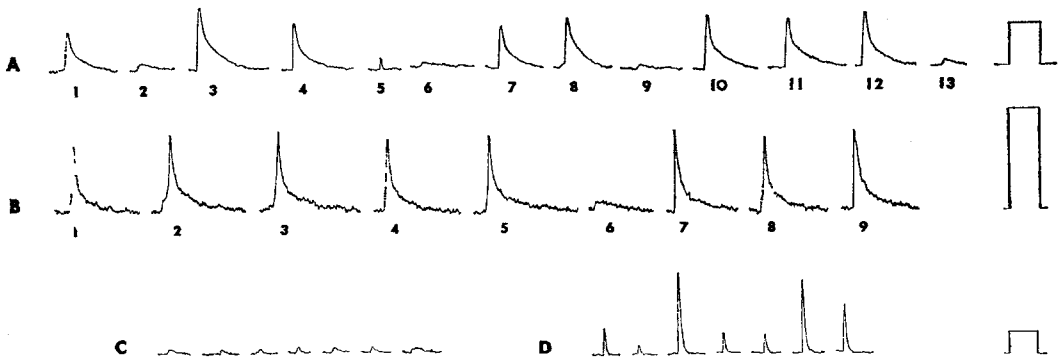


FIGURE 1. Isolated discrete waves in two different retinula cells and in one eccentric cell. An isolated discrete wave is one which is not overlapped in time by any other. A, first 13 isolated discrete waves during a run in a retinula cell arranged in the order of their appearance. B, first nine isolated discrete waves from an eccentric cell. C, the first seven isolated S waves, and D the first seven isolated L waves in one retinula cell. A, retinula cell, 15°C. B, eccentric cell, 14°C. C and D, retinula cell, 14°C. All calibration marks, 5 mv, 1 sec. A, waves 2, 6, 9, and 13, S waves. B, wave 6, S wave. All others, L waves.

bimodal but for the one representing the eccentric cell (Fig. 2 B) the modes are sharply defined and there is no overlap between them, while for the histogram (A) representing the retinula cell the modes are broader and there is substantial overlap between them. Thus, in general, discrete waves could not be classified into mutually exclusive categories on the basis of their peak amplitudes alone. Moreover, such a classification, with reference to Fig. 1 A, (e.g. greater or less than 2.5 mv) would include discrete waves 5 and 6 in the same category.

These findings suggested that discrete waves might be better classified on the basis of their time courses as well as their peak amplitudes. We defined an

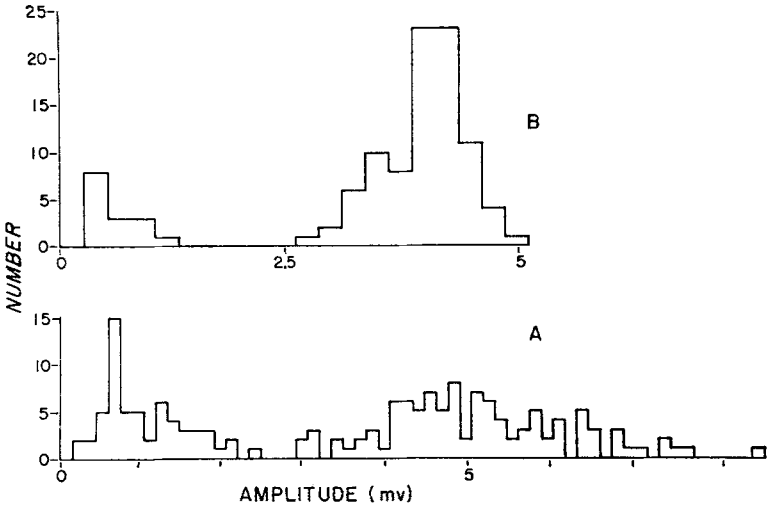


FIGURE 2. Amplitude distributions of discrete waves for two different cells. Ordinates, number of discrete waves with peak amplitude equal to that shown on abscissa. A, retinula cell, 15°C. B, eccentric cell, 14°C.

L wave as one which had a rapid rise and a rapid decline, and which was usually large, and we defined an S wave as one which had a slow rise, and a slow decline and which was always small. Waves 2, 6, 9, and 13 in Fig. 1 A and wave 6 in Fig. 1 B were classified as S waves. All the other waves in Figs. 1 A and 1 B were designated L waves (including wave 5 of Fig. 1 A). The terms large, small, rapid, and slow were defined relative to the population of discrete waves studied. For the cell shown in Figs. 1 A and 2 A, large and small were defined as greater than and less than 2.5 mv. It is clear from Fig. 1 A that we could have also defined rapid and slow quantitatively, but the distinction was unambiguous by simple inspection.

In some retinula cells, the variability of the peak amplitudes of the L waves was greater than that shown in Fig. 1 A. For example, Fig. 1 D shows isolated L waves from a different retinula cell. The figure was constructed by selecting

the first seven isolated L waves in the run. Fig. 1 C shows seven isolated S waves from the same run.

The uniformity of the appearance of L waves in Fig. 1 B is typical of the eccentric cells we studied. In addition, the areas under the voltage–time curve of 100 L waves from each of three eccentric cells were measured, and the fractional variation (standard error/mean) of the area was estimated as approximately 0.15. We emphasize these findings because they suggest that L waves are quasi all-or-nothing responses.

Fig. 3 A, B, C, D, E, and F show representative examples of an S and L wave from the same run for six different retinula cells. The properties that characterize the two wave types are evident in each example. There was considerable variation of the sizes and shapes of S and L waves from cell to cell even at similar temperatures (e.g. compare Fig. 3 D with Fig. 3 E). There was also a systematic slowing of both wave types as the temperature was decreased (e.g. compare Fig. 3 B with Fig. 3 C).

Fig. 4 is a graph of the log of the amplitude of the average of 10 L waves from a single eccentric cell. Time $t = 0$ corresponds to the peak of the average L wave. It is apparent that the L waves had two phases of exponential decline. Fig. 3, A thru F, shows that the time course of the second phase of decline of each L wave was similar to the time course of the decline of the S wave from the same run.

*Slow Depolarizations Preceding L Waves*

Fig. 3 G shows L waves that were preceded by a slow depolarization. Similar slow depolarizations can be seen in Fig. 1 A wave 8, and Fig. 1 B wave 2. We were able to find similar examples in almost every retinula and eccentric cell studied. Of the great majority of L waves that were not preceded by a slow depolarization, some had a slight inflection on their rising phase as in Fig. 1 A wave 10, Fig. 2 A wave 7, Fig. 3 A, and Fig. 3 E. Slow depolarizations of the type shown in Fig. 3 H were previously reported by Adolph (1964), and by Borsellino and Fuortes (1968).

The slow depolarization preceding an L wave might be interpreted as the occurrence of an L wave during the time course of an S wave. If in addition, the occurrence of either an S wave or an L wave was an independent event, then it would be possible to predict the number of L waves that were preceded by a slow depolarization from the probabilities of the occurrence of each type alone. For example, in an eccentric cell, we observed spontaneous waves for a period of 5 min and during that period, each discrete wave was isolated. The record contained 78 discrete waves, of which 67 were L waves, 11 were S waves, and 9 of the 67 L waves were preceded by a slow depolarization. The average duration of an S wave was approximately 0.2 sec. Thus, the conditional probability that an L wave begins within 0.2 sec following the onset of an S wave

was calculated as approximately 0.01, and the total number of S waves was 20 (9 + 11). The expected number of L waves preceded by a slow depolarization was calculated as 0.2 for the 5 min observation period. Since the observed number of the last category was 9, it follows that the slow depolarization was not the temporal coincidence of an S wave and an L wave. We also note that a slow depolarization preceding an L wave was almost always progressive.

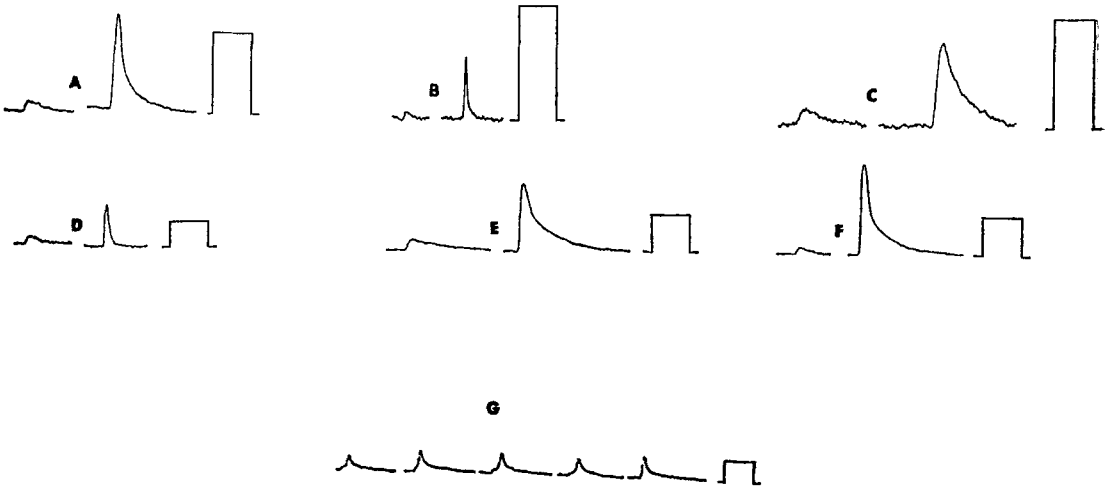


FIGURE 3, A–F. Isolated S and L waves. An isolated S wave and an isolated L wave is shown, in that order, for each of six different retinula cells. A, 13°C, B, 19°C, C, 8.5°C, D, 10.5°C, E, 12.5°C, F, 14°C, G, five L waves from a single eccentric cell. Each is preceded by slow depolarization. 14°C. All calibrations, 5 mv, 1 sec.

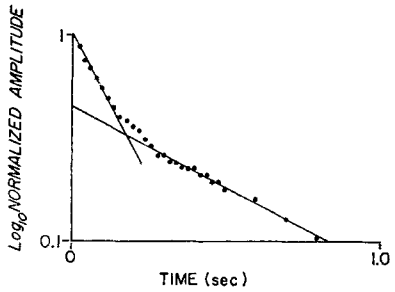


FIGURE 4. Decline of L wave from its peak. Average of 10 L waves from a single run. Ordinate, $\log_{10}$ (amplitude/peak amplitude). Abscissa, time, $t = 0$ corresponds to the peak of the average L wave. Eccentric cell, 14°C.

### *The Numbers of S and L Waves*

The ratio of L to S waves was variable from cell to cell and ranged from 3 to 10. The number of L waves that followed a brief flash of light of fixed (average) energy also varied from trial to trial. If each photon absorbed resulted in either precisely one L wave, or in no L wave at all, then the number of L

waves would be expected to vary from trial to trial according to the individual terms of the Poisson distribution. But if each photon absorbed resulted in more than one L wave, then this would not be true. We studied this question in several cells as follows. An interstimulus interval was divided into two successive epochs each 2.5 sec in duration (in order to partially separate light-induced and spontaneous L waves). Let $N$ equal the number of trials in a run and let $N_k$ (for $k = 0, 1, 2, \cdots$) equal the number of trials on which exactly $k$ L-waves were observed during an epoch. Then, the expected values of $N_k$ were calculated from $N_k = N(\bar{N}^k/k!) \exp(-\bar{N})$ where $\bar{N} = -\log_e(N_0/N)$. The observed and expected values of $N_k$ are tabulated in Table I below. It is clear from the table that the distribution of the numbers of L waves did follow the individual terms of the Poisson distribution, for both epochs of each run.

TABLE I

OBSERVED AND EXPECTED VALUES OF $N_k$

| | Cell 1 | | | | Cell 2 | | | | Cell 3 | | | |
|---|---|---|---|---|---|---|---|---|---|---|---|---|
| | Epoch 1 | | Epoch 2 | | Epoch 1 | | Epoch 2 | | Epoch 1 | | Epoch 2 | |
| | *o* | *e* | *o* | *e* | *o* | *e* | *o* | *e* | *o* | *e* | *o* | *e* |
| $N$ | 240 | — | 240 | — | 278 | — | 278 | — | 197 | — | 197 | — |
| $N_0$ | 121 | — | 169 | — | 135 | — | 256 | — | 166 | — | 184 | — |
| $N_1$ | 84 | 84 | 59 | 57 | 98 | 97 | 21 | 21 | 30 | 28 | 13 | 13 |
| $N_2$ | 31 | 28 | 11 | 10 | 30 | 36 | 1 | 1 | 1 | 1 | 0 | 0 |
| $N_3$ | 4 | 6 | 1 | 1 | 13 | 8 | 0 | 0 | 0 | 0 | 0 | 0 |
| $N_4$ | 0 | 1 | 0 | 0 | 2 | 3 | 0 | 0 | 0 | 0 | 0 | 0 |

*o*, observed; *e*, expected.

### *The Latency of Discrete Waves*

Fig. 5 A shows the latency distribution of isolated S waves and the latency distribution of the slow depolarization that (sometimes) preceded an L wave. Fig. 5 B shows separately the latency distributions of L waves which were, or were not preceded by a slow depolarization. The latency measurement shown in Figs. 5 A and 5 B are all from the same run. It is clear from these figures, that all the latency distributions are similar. Fig. 5 C shows that the time elapsed between the detection of the slow depolarization and the beginning of an L wave was short compared to the latency itself. The value plotted at time $t = 0$ is the number of L waves for which there was no preceding slow depolarization. However, some of the latter L waves did have an inflection on their rising phase. Fig. 5 shows that it was reasonable to combine all latency measurements.

Figs. 6 A and 6 B are representative estimates of $z(k)$ from a single retinula cell at two different temperatures. The best estimates of $m$ and $\alpha$ in equation

(6) were determined as described in the methods section and the predicted values of $z(k)$ were calculated from these estimates using expression (9). In Figs. 6 A and 6 B the point symbols show the predicted values. For Fig. 6 A the best estimates of $m$ and $\alpha$ were 18.2 and 97.2 per sec respectively. For Fig. 6 B, the best estimates of $m$ and $\alpha$ were 17.4 and 32.6 per sec respectively. The quality of the fit shown in Figs. 6 A and 6 B is typical of the 108 runs studied.

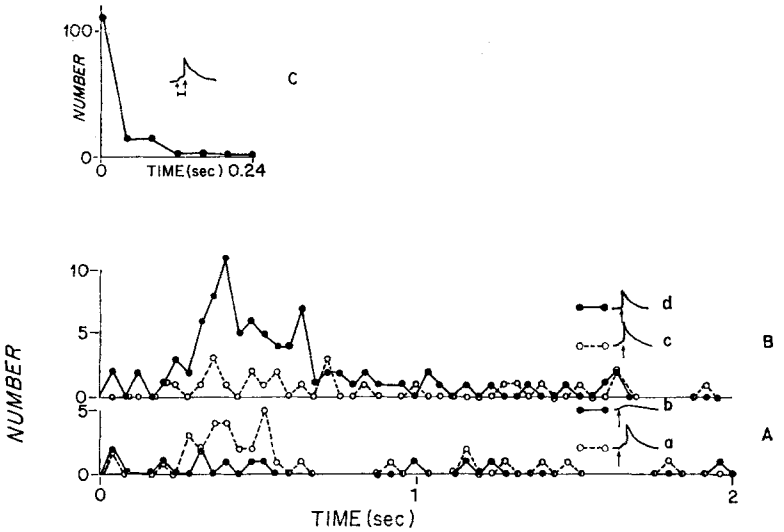


FIGURES 5 A and 5 B. Latency distribution of first discrete wave to follow a brief flash of light. Ordinates, number of discrete waves with latency equal to that shown on abscissa. Time $t = 0$ corresponds to the beginning of the flash. Inserts, arrow shows when in time course of the discrete wave the latency was measured, and the plotting symbol used in the graph is indicated. 5 C, distribution of elapsed time between detection of slow depolarization and onset of rapid rising phase of L wave. (See insert.) Ordinate, number of discrete waves for which time elapsed was that shown on abscissa. Value of ordinate at $t = 0$, number of L waves with no detectable preceding depolarization. All graphs from the same run. Eccentric cell, 14°C.

Fig. 6 C shows that the time corresponding to the maximum value of $z(k)$ was increased when the temperature was decreased. Figs. 6 A and 6 B show typical examples of the estimate, $z(k)$ for one cell at two different temperatures. There was considerable variation in the shape of the latency distributions from cell to cell. This was reflected by large variations in the estimates of $\alpha$ and $m$ for different cells at the same temperature. For example, for seven cells, and at temperatures ranging from 14°C to 15°C, the estimates of $m$ ranged from 6.26 to 18.89, with mean value 12.79, and fractional valuation 0.38. The variation in the estimate of $m$ was about four times the error of the

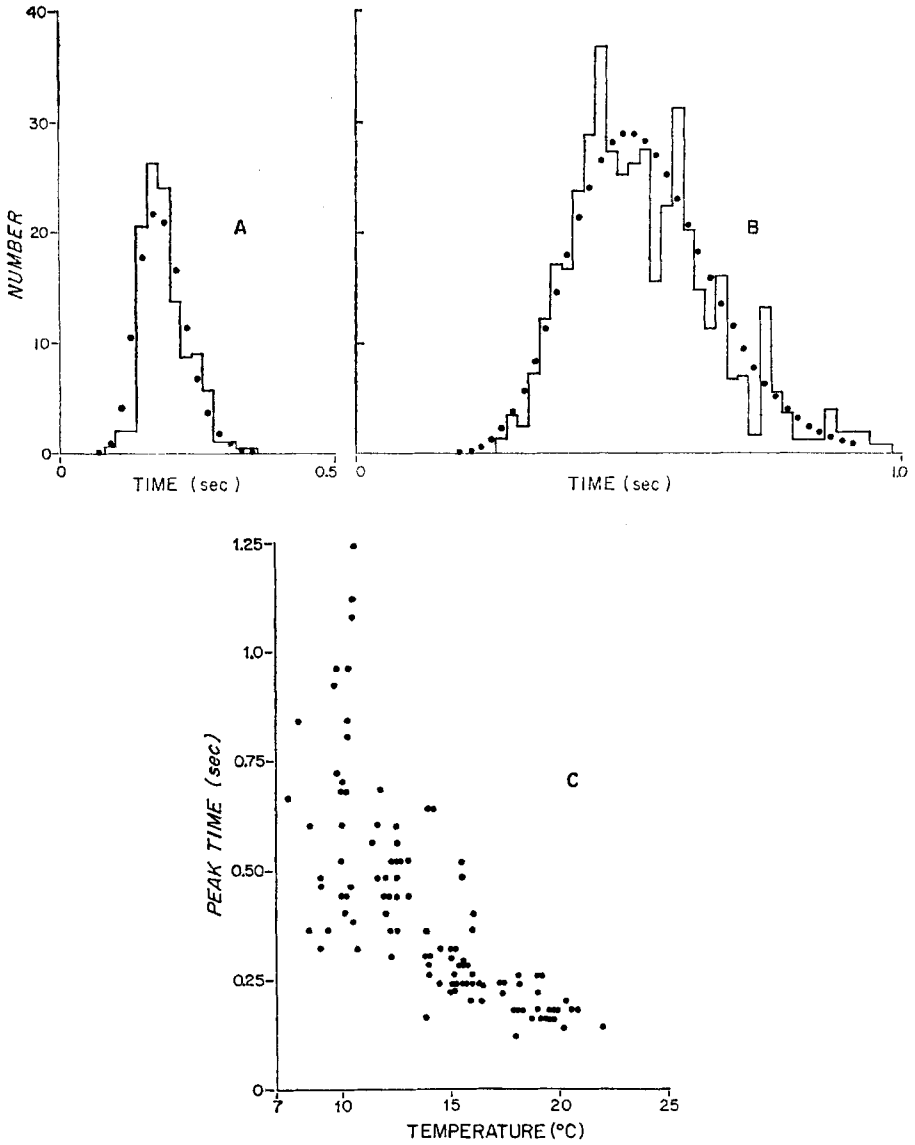


FIGURES 6 A and 6 B. Predicted and observed estimates of $z(k)$. (See text.) Histograms, observed. Point symbols, predicted. Ordinates, values of $z(k)$. Abscissa, time. Time $t = 0$, corresponds to the beginning of a 10 msec flash. The graphs are for the same retinula cell. A, 19°C. B, 9°C. C, time to reach peak value of $z(k)$ vs. temperature. Ordinate, time to peak. Abscissa, temperature. Values for 108 runs on 33 different cells.

method. Similar results were obtained with regard to $\alpha$. In order to determine the effect of temperature, it was, therefore, necessary to study each cell separately. In 18 cells, runs were obtained at two or more temperatures. For each of these cells, linear regression slopes for the estimates of $m$ and $\alpha$ against

temperature were calculated. If the variation in the estimates of $m$ and $\alpha$ were due to chance, equal numbers of positive and negative slopes would have resulted. However, in 16 of the 18 cells, the regression slope for $m$ against temperature was positive, and in 14 of the 18 cells the regression slope for $\alpha$ against temperature was positive. It was calculated from the binomial distribution, that at least 16 of 18 of the slopes might have been positive simply due to chance with a probability 0.0027, and at least 14 of 18 slopes might have been positive with a probability 0.064. Therefore, it is likely that $m$ and $\alpha$ changed systematically with temperature.

*Estimates of $\mu$ and $\alpha$*

In each of 19 runs on 13 cells, and at temperatures ranging from 7.5° to 19.5°C, we compared the estimate of $\alpha$ made as already described, to an estimate of $\mu$ obtained by fitting an exponential curve to the second (slow) phase of decline of isolated L waves observed during the run (as in Fig. 4). In the derivation of the *p.d.f.* of the latency of discrete waves, we assumed that $\alpha$ was much larger than $\mu$, so that a comparison of these estimates provided a check on this approximation. Table II, summarizes the results. On the average, $\alpha$ was about 17 times as large as $\mu$.

TABLE II

ESTIMATE OF $\alpha$ AND $\mu$

| Cell | Temperature | $\alpha$ | $\mu$ |
|---|---|---|---|
| | °C | $sec^{-1}$ | $sec^{-1}$ |
| 1 | 9.0 | 43 | 1.5 |
| 1 | 12.0 | 72 | 4.5 |
| 1 | 19.0 | 98 | 4.9 |
| 2 | 7.5 | 22 | 2.0 |
| 3 | 15.6 | 93 | 4.5 |
| 4 | 8.5 | 17 | 1.8 |
| 4 | 11.8 | 14 | 8.2 |
| 5 | 14.0 | 59 | 1.7 |
| 5 | 19.5 | 156 | 3.2 |
| 6 | 13.0 | 25 | 2.0 |
| 6 | 18.0 | 83 | 1.9 |
| 7 | 15.5 | 26 | 2.1 |
| 8 | 12.0 | 22 | 6.1 |
| 9 | 15.0 | 32 | 5.3 |
| 10 | 9.8 | 43 | 2.9 |
| 10 | 12.5 | 55 | 1.9 |
| 11 | 14.0 | 18 | 2.4 |
| 12 | 13.0 | 79 | 2.8 |
| 13 | 15.7 | 45 | 8.2 |

*Discussion and Conclusions*

The results presented support our model as follows.

(*a*) We found two distinct and mutually exclusive classes of discrete waves, namely S waves and L waves. It is necessary, however, to consider that this observation might have resulted from the electrical coupling among the cells of the ommatidium (Borsellino, Fuortes, and Smith, 1965). Thus, L waves might have originated in the same retinula cell that contained the microelectrode, while S waves might have originated in the other retinula cells of the ommatidium. The arrangement of the retinula cells about the dendrite of the eccentric cell is symmetrical (Miller, 1957), and this suggests that if electrical coupling were the only cause of S and L waves, a single class would be observed with a microelectrode in an eccentric cell. However, we found that both S and L waves were easily detected in eccentric cell preparations. Our results suggest that both types were generated only in retinula cells, and that electrical coupling among the cells of the ommatidium caused the greater inhomogeneity of L waves in retinula cells than in eccentric cells.

(*b*) In eccentric cells, L waves were uniform in appearance, and in either eccentric or retinula cells they were sometimes preceded by a slow depolarization. These observations suggest that L waves represent the propagated responses of our model, and that S waves represent the occasional instances when a propagated response fails.

(*c*) The time courses of the L waves and S waves were similar to those predicted by our model. In particular, we attribute the rapid rise and the first (rapid) decline of the L wave to voltage and time-dependent properties of the photoreceptor membrane analogous to the all-or-nothing response of axonal membrane. The decline of the S waves was similar to the second (slow) phase of the L wave decline, in agreement with our model and we attribute both declines to the same exponential decay of open sodium channels. The rising phase of the S wave had a time course, on the average, similar to the prediction of equation (3), but the number of isolated S waves was too few, and their resolution too poor, to permit quantitative comparison.

(*d*) Using methods described earlier, we estimated the *p.d.f.* of the latency of the response to a single photon, and this estimate was well described by the gamma density of equation (6). For single runs, the estimate of $\alpha$ made from the latency distribution was, on the average, 17 times larger than the estimate of $\mu$ made from the second (slow) phase of decline of representative L waves. This supports the approximation we used in the theory section. The latency distributions of S waves and L waves were similar, and therefore, were combined on the justification of empirical evidence. It would have been more accurate to use only the latencies of the L waves to estimate $\alpha$. However, the peak amplitude distributions of S and L waves often overlapped and thus

no simple and reliable procedure, other than visual discrimination, could be found to separate them. Because of the large number of latency measurements that were required, hand analysis was not practical.

In further support of the assumption that propagated responses occur in the *Limulus* photoreceptor, we discuss certain properties of the ventral photoreceptor cell. Millecchia and Mauro (1969), showed that the ventral photoreceptor cells of *Limulus* have properties similar to retinula cells. Using a voltage clamp, they found that the cell conductance increased in response to light and that the time course of the increase mimicked the response of the unclamped cell to light. Discrete waves were observed in clamped and unclamped conditions. The unclamped response of the cell to a moderately intense flash of light was similar to that observed in the lateral eye (Yeandle, 1967), and consisted of a sharp depolarization called a spike (or a regenerative response, but not to be confused with an action potential), followed by a slower transient depolarization. When the cell was voltage clamped, the conductance change had no component analogous to the spike. We assume that the retinula cell behaves similarly, and that its response results from the superposition and interaction of discrete waves (Dodge, Knight, and Toyoda, 1968). Thus, the spike may reflect the occurrence of L waves. This suggests that L waves do not occur in the voltage-clamped condition, and supports our assumption of a critical depolarization.

In the theory section, we assumed that when two or more photons were absorbed coincidently, they acted independently with regard to latency. This allowed us to use the results of Srebro and Yeandle (1970) to calculate the latency distribution for a single photon absorption from experiments in which more than one photon might have been absorbed during a brief flash of light. It is implicit in the assumption, that summation of depolarization among sites of simultaneously absorbed photons was negligible. We justify this assertion as follows. In our experiments the number of photons absorbed on each trial was, on the average, one per trial. Thus, on approximately 90% of the trials, two or fewer photons were actually absorbed. If photons were absorbed uniformly along the rhabdome, then two simultaneously absorbed photons were separated, on the average, by one-half the length of the rhabdome. Moreover, the photons were absorbed by different retinula cells. Under these restrictive conditions, it seems reasonable that the depolarization due to the direct effect of one photon absorption, had a negligible summative effect on the direct action of a second coincidently absorbed photon.

Two experimental observations do not support our model. (*a*) The discrete wave process is not affected by tetrodotoxin (Dodge, Knight, and Toyoda, 1968). (*b*) The response of the ventral photoreceptor cell to light is only temporarily abolished by perfusion with sodium-free solutions (Millecchia and Mauro, 1969). With regard to the first observation, we note that there

are obvious differences, as well as similarities between the sodium conductance mechanisms of the *Limulus* photoreceptor and the axon. For example, the sodium conductance changes are much slower in the photoreceptor than they are in the axon. It seems reasonable that the pharmacological properties may also differ. The second observation suggests that sodium may not be the only ion involved in the production of photocurrent. But there is much evidence to support the hypothesis that sodium is the major current carrier when the photoreceptor is in normal sea water (Millecchia and Mauro, 1969).

Our description of S and L waves is similar to that of Borsellino and Fuortes (1968), and we used their nomenclature. However, we found that the latency distributions of the two types of waves were essentially the same, while they found dramatic differences. Srebro and Yeandle (1970) reported that there was only a slight correlation between the amplitude and the latency of the first discrete wave to follow a light stimulus. Their finding is similar to our results.

Recently, a stochastic compartment model was proposed to account for the behavior of discrete waves in the *Limulus* photoreceptor (Borsellino and Fuortes, 1968). In this model, the absorption of a single photon results in the instantaneous injection of a single "particle" into an initial "compartment." Particles multiply along a stochastic chain of $n$ compartments. The arrival of a particle in the $n^{th}$ compartment results in an "elementary" depolarization, and the temporal pattern of the arrival of particles in the $n^{th}$ compartment determines the time course of the S wave. Each particle that arrives in the $n^{th}$ compartment has a small fixed probability of generating an L wave. The authors suggest that the model may represent a sequence of $n$ chemical reactions. They do not specify how spontaneous discrete waves occur or how a particle generates an L wave. However, they corrected their observed latency distributions for S and L waves by "subtracting the probability that the same type of wave occurred in darkness" (Borsellino and Fuortes, 1968, p. 527, Fig. 15, caption), a procedure that implies that spontaneous and light-induced discrete waves are not independent.

The following properties of discrete waves can be deduced from both the compartment model and from our model: (*a*) there are two types of discrete waves, similar to S and L waves, (*b*) a slow depolarization may precede an L wave, (*c*) the latency of the S wave has a *p.d.f.* given by a gamma density function similar to equation (6).

The following important differences exist between the compartment model and our model.

(*a*) In the compartment model each particle arriving at the $n^{th}$ compartment has a fixed probability of generating an L wave. More than one L wave may, therefore, result from a single photon absorption. Experiments

already reported (Fuortes and Yeandle, 1964) as well as the data we presented strongly suggest that only one L wave (may) result from a single photon absorption.

(*b*) In the compartment model the latency of the S wave must be shorter than the latency of the L wave. In our model, the latency of the S wave depends on its amplitude relative to the noise of the electrode. In general, the latency of the S wave may be either longer or shorter than the latency of the L wave, but our data show that their latencies are, in fact, similar.

(*c*) In the compartment model, the number of compartments is a fixed property of the cell and it is thought to represent the number of chemical reactions intervening between the absorption of a photon and the elementary depolarization. The latency of the S wave has a gamma density function with shape parameter, $n$, simply related to the number of compartments. In our model, all discrete waves have similar latency with *p.d.f.* given by a gamma density whose shape factor, $m$, is simply related to the critical depolarization required to initiate a propagated response. Thus, $m$ is, in general, variable from cell to cell, and may change with temperature in a single cell. Our data suggest that both the shape factor, $m$, and rate constant, $\alpha$, change systematically with temperature in a single cell and vary appreciably from cell to cell.

(*d*) In the compartment model, "amplification" occurs in the sense that a single photon injects a single particle into the initial compartment but results in a larger number of particles in the last compartment. If the compartments represent a sequence of chemical reactions, this implies an enzyme amplifier mechanism (Borsellino, Fuortes, and Smith, 1965). There is no evidence that such a process exists in any other neuronal membrane. In our model, "amplification" occurs in the sense that the absorption of one photon may effect the opening of numerous sodium channels. The first stage of the process is somewhat novel in that the gating mechanism is stochastic, but the initiation of a propagated response is a typical property of neuronal membrane.

Bass and Moore (1970) proposed that a photon absorption simply opens a single sodium channel in the rhabdomere membrane, and that a propagated response results from the ensuing depolarization. Their model does not explain the stochastic properties of discrete waves.

Levinson (1966) proposed a model for the response of the *Limulus* photoreceptor in which "particles pelt" the photoreceptor membrane at a steady rate, and collect at the site of a photon absorption. Depolarization occurs when a critical number of particles collect. In our model, the opening of sodium channels plays a role similar to Levinson's particles with regard to latency.

This work was supported by U. S. Public Health Service Grant EY00435 from the National Eye Institute.

*Received for publication 15 February 1971.*

## BIBLIOGRAPHY

ADOLPH, A. R. 1964. Spontaneous slow potential fluctuations in the *Limulus* photoreceptor. *J. Gen. Physiol.* **48**:297.

BASS, L., and W. J. MOORE. 1970. An electrochemical model for depolarization of a retinula cell of *Limulus* by a single photon. *Biophys. J.* **10**:1.

BORSELLINO, A., and M. G. F. FUORTES. 1968. Responses to single photons in visual cells of *Limulus*. *J. Physiol. (London).* **196**:507.

BORSELLINO, A., M. G. F. FUORTES, and T. G. SMITH. 1965. Visual responses in *Limulus*. Cold Spring Harbor Symp. Quant. Biol. **30**:429.

DODGE, F. A., B. W. KNIGHT, and J. TOYODA. 1968. Voltage noise in *Limulus* visual cells. *Science (Washington).* **160**:88.

DRAPER, N. R., and H. SMITH. 1966. Applied Regression Analysis. John Wiley & Sons Inc., New York.

FELLER, W. 1957. An Introduction of Probability Theory and Its Applications. John Wiley & Sons Inc., New York. **1**:414.

FUORTES, M. G. F. 1959. Initiation of impulses in visual cells of *Limulus*. *J. Physiol. (London).* **148**:14.

FUORTES, M. G. F., and S. YEANDLE. 1964. Probability of occurrences of discrete potential waves in the eye of *Limulus*. *J. Gen. Physiol.* **47**:443.

HECHT, S., S. SHLAER, and M. H. PIRENNE. 1942. Energy, quanta, and vision. *J. Gen. Physiol.* **25**:819.

HODGKIN, A. L., and A. F. HUXLEY. 1952. A quantitative description of membrane current and its application to conduction and excitation in nerve. *J. Physiol. (London).* **117**:500.

KIKUCHI, R., K. NAITO, and I. TANAKA. 1962. Effect of sodium and potassium ions on the electrical activity of single cells in the lateral eye of horseshoe crab. *J. Physiol. (London).* **161**:319.

LEVINSON, J. 1966. One-stage model for visual temporal integration. *J. Opt. Soc. Amer.* **56**:95.

MARKOVIC, R. D. 1965. Probability functions of best fit to distributions of annual precipitation and runoff. Hydrology Papers Colorado State University. Fort Collins, Colorado. No. 8.

MILLECCHIA, R., and A. MAURO. 1969. Ventral photoreceptor cells of *Limulus*. III. A voltage-clamp study. *J. Gen. Physiol.* **54**:331.

MILLER, W. H. 1957. Morphology of the Ommatidia of the compound eye of *Limulus*. *J. Biophys. Biochem. Cytol.* **3**:421.

REICHARDT, W. E. 1965. Quantum sensitivity of light receptors in the compound eye of the fly *Musca*. *Cold Spring Harbor Symp. Quant. Biol.* **30**:505.

SMITH, T. G., and J. E. BROWN. 1966. A photoelectric potential in invertebrate cells. *Nature. (London).* **212**:1217.

SMITH, T. G., W. K. STELL, and J. E. BROWN. 1968. Conductance changes associated with receptor potentials in *Limulus* photoreceptors. *Science (Washington).* **162**:454.

SREBRO, R., and S. YEANDLE. 1970. Stochastic properties of discrete waves of the *Limulus* photoreceptor. *J. Gen. Physiol.* **56**:751.

WOLBARSHT, M. L., and S. YEANDLE. 1967. Visual processes in the *Limulus* eye. *Annu. Rev. Physiol.* **29**:531.

YEANDLE, S. S. 1967. Some properties of the components of the *Limulus* ommatidial potential. *Kybernetik.* **3**:250.